

Influences of Annealing Temperature on the Optical and Structural Properties of Manganese Oxide Thin Film by Zn Doping from Sol–Gel Technique

S. PISHDADIAN* AND A.M. SHARIATI GHALENO

Department of Physics, Shahrood Branch, Islamic Azad University, Shahrood, Iran

(Received February 26, 2012)

Thin films of MnO_2 , Mn_2O_3 , and Mn_3O_4 have been grown from single precursor solution by varying the post-annealing condition on the glass and corning substrate using a sol–gel technique. By annealing in air and at temperature between 600 and 800 °C, cubic Mn_2O_3 films could be formed. The films were thermally annealed at different temperatures between 300 and 800 °C to create different crystalline structure. Even under the air-annealing condition, Zn doping results in a structural transformation from cubic $\text{Zn}_x\text{Mn}_{2-x}\text{O}_3$ to tetragonal $\text{Zn}_x\text{Mn}_{3-x}\text{O}_4$. X-ray diffraction, atomic force microscopy, and UV-visible spectra were used to characterize the effect of thermal annealing on the optical and structural properties of a Zn doped manganese oxide thin film. Optical properties of the Mn_2O_3 and Mn_3O_4 films have been investigated by pointwise unconditioned minimization approach.

DOI: [10.12693/APhysPolA.123.741](https://doi.org/10.12693/APhysPolA.123.741)

PACS: 78.66.–w, 81.10.–h, 68.55.Jk

1. Introduction

Manganese oxide is a transition metal oxide. Cubic Mn_2O_3 , tetragonal Mn_3O_4 and cubic MnO structures could be obtained from MnO_2 by varying the post-annealing conditions. Among these oxides, MnO_2 is most stable. Such varieties in their structures and hence in physical and chemical properties make them attractive to study their fundamental physical properties and technological applications. Thin films of manganese-based oxide can be potentially used as rechargeable batteries, catalysts, electrochemical capacitors, sensors and magnetoelectronic devices. Various structural, electronic, and magnetic properties of manganese-based oxides are mainly affected by various oxidation conditions and locations of the manganese ions in the unit cell of these oxides. Different methods have been employed to fabricate manganese oxide thin films, such as sputtering [1, 2], electron beam evaporation [3], pulse laser deposition [4, 5], molecular beam epitaxy [6, 7], electrochemical [8], spray pyrolysis [9, 10] and sol–gel [11, 12]. Although the structural, electronic and magnetic properties of manganese oxide have been well investigated, to the author's knowledge, their optical properties have hardly been investigated so far. In this work, various manganese oxide films have been prepared by sol–gel, employing dip-coating method. Mn_2O_3 and Mn_3O_4 structures could be obtained by changing the annealing condition. Also, a structural transformation from Mn_2O_3 to Mn_3O_4 was observed by Zn doping. The effects of annealing on the structural and optical constants were investigated.

2. Experimental

MnO_2 , Mn_2O_3 and Mn_3O_4 films were deposited on soda lime and corning substrate by sol–gel employing dip-coating method. The sol was prepared by dissolving $\text{Mn}(\text{CH}_3\text{COO})_2 \cdot 4\text{H}_2\text{O}$ as precursor and monoethanolamin (MEA) as complexing agents and 2-methoxyethanol as solvent. The mixture was stirred at 80 °C for 3 h. For Zn doping, $\text{Zn}(\text{C}_2\text{H}_5)_2 \cdot 2\text{H}_2\text{O}$ and $\text{Mn}(\text{CH}_3\text{COO})_2 \cdot 4\text{H}_2\text{O}$ powders were dissolved together. The coating solutions were aged for one day at room temperature, and then were dip-coated on the substrate. Resulted thin film was heated at 90 °C for 5 min after each deposition. This process was repeated seven times to increase the film thickness. After drying, these films were annealed at 300–800 °C in air for 4 h. An X-ray diffractometer (B8-advance Bruker axs) was used to determine the crystallite structure of the films. Detailed morphological analysis of the manganese oxide thin films was carried out by atomic force microscopy (AFM) using a Dual Scope Microscope model DME 2401. Normal-incidence transmittance was measured over the wavelength range 300–1000 nm using a Himadzu Uv-1800 spectrophotometer. The idea of assuming a closed formula for n and k depending on few coefficients has been exploited in celebrated methods. The methods originated on this idea are efficient when the transmittance curve exhibits some fringe patterns, representing rather large zones of the spectrum where $k(\lambda)$ is almost null. The transmission of a thin absorbing film deposited on a thick transparent substrate is given by

$$T = \frac{Ax}{B - Cx + Dx^2}. \quad (1)$$

Instead of imposing a functional form for $n(\lambda)$ and $k(\lambda)$, the phenomenological constraints that restrict the variability of these functions were stated explicitly so that

*corresponding author; e-mail:
spishdadian@iau-shahrood.ac.ir

the estimation problem is formed as follows:

$$\text{Minimize} \sum |\text{Theoretical } T(\lambda) - \text{Measured } T(\lambda)|^2. \quad (2)$$

In this way, well behaved functions $n(\lambda)$ and $k(\lambda)$ can be obtained without severe restrictions that may damage the quality of the fitting [13]. In this paper, the optical constants and the thickness of thin films were estimated by recent method.

3. Results and discussion

The manganese oxide films showed amorphous phase with no observable X-ray diffraction (XRD) peak when the annealing temperature was less than 500 °C. As shown in Fig. 1, annealing the deposited films in air and also at 600–800 °C for 4 h led to good-quality formation of Mn_2O_3 . The XRD data for the films exhibit characteristic peaks for Mn_2O_3 without any other phases. The estimated cubic lattice constant of the Mn_2O_3 film is 9.36 Å, which is quite close to 9.40 Å that was reported for bulk Mn_2O_3 [14]. When Zn was added in the precursor solution, a structural transformation was observed from cubic Mn_2O_3 to tetragonal Mn_3O_4 even under the same air-annealing condition. Figure 2 shows that the XRD spectrum of Zn-doped Mn_2O_3 film looks quite similar to that of pure Mn_2O_3 . This film can be described as $\text{Zn}_x\text{Mn}_{2-x}\text{O}_3$ with $x = 0.06$.

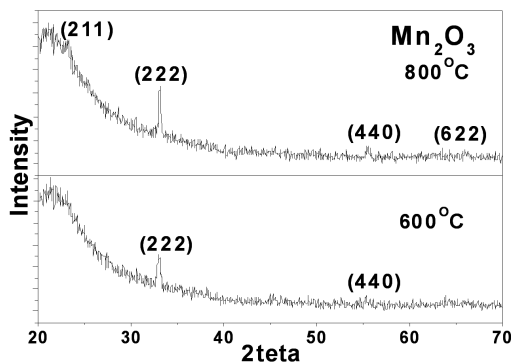


Fig. 1. XRD spectra of manganese oxide films obtained by air-annealing at 300–800 °C for 4 h.

The estimated cubic lattice constant of the Mn_2O_3 film from $\text{Zn}_x\text{Mn}_{2-x}\text{O}_3$ with $x = 0.06$ is 10.26 Å. However, it is shown that the Zn-doped Mn_2O_3 film also contains minor Mn_3O_4 -like phase as marked by * in Fig. 2. By increasing the Zn content in the precursor solution as $\text{Zn}_x\text{Mn}_{3-x}\text{O}_4$ with $x = 0.16$ –0.36 the resulted films exhibit complete Mn_3O_4 like phase at 600–800 °C as shown in Fig. 3. The films which were annealed at the temperature below the 600 °C were amorphous. The estimated tetragonal lattice constants of Mn_3O_4 film are $a = 6.44$ Å and $c = 10.24$ Å, which are in agreement with previously reported values of 5.760 and 9.440 Å, respectively, in case of bulk Mn_3O_4 [15]. The effects of annealing temperature on the surface morphology of $\text{Zn}_x\text{Mn}_{3-x}\text{O}_4$ ($x = 0.36$) films are clearly evidenced in Fig. 4. The surfaces of the

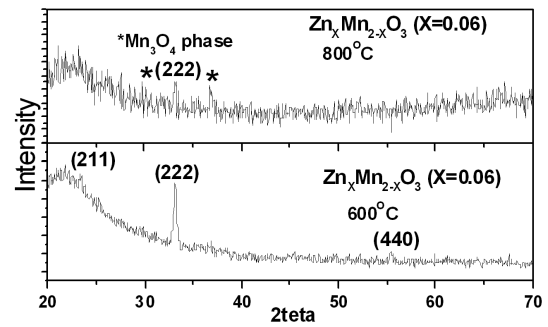


Fig. 2. XRD spectra of $\text{Zn}_x\text{Mn}_{2-x}\text{O}_3$ ($x = 0.06$) obtained by air-annealing at 600 and 800 °C for 4 h.

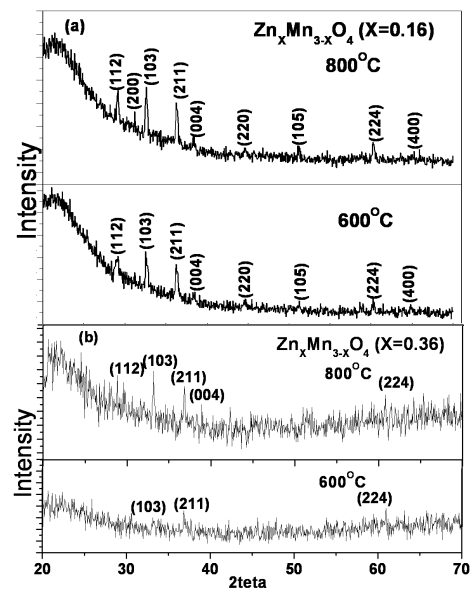


Fig. 3. XRD spectra of $\text{Zn}_x\text{Mn}_{3-x}\text{O}_4$: (a) $x = 0.16$ and (b) $x = 0.36$ obtained by air-annealing at 600 and 800 °C for 4 h.

films show crack free areas in the explored section. Manganese oxides which were annealed at 300 °C and 400 °C exhibit different appearance (see Fig. 4a and b). The film which was annealed at 400 °C shows the smaller grains and hence has lower roughness and thickness than the film which was annealed at 300 °C. At 500 °C, the significant change in morphology could be caused by crystallization of the amorphous MnO_2 , since the corresponding formation of crystalline Mn_3O_4 . As the annealing temperature is raised to 600 °C, the oxide morphology becomes islands (as shown in Fig. 6d). The morphology of the oxide which was annealed at temperatures higher than 600 °C is presented in Fig. 6e. Oxide corresponding to the phase transformation to Mn_3O_4 (from XRD) can be observed.

Figures 5–8 show the optical transmittance spectra of manganese oxide and $\text{Zn}_x\text{Mn}_{2-x}\text{O}_3$ with $x = 0.06$ and $\text{Zn}_x\text{Mn}_{3-x}\text{O}_4$ ($x = 0.16$ –0.36) films which were annealed

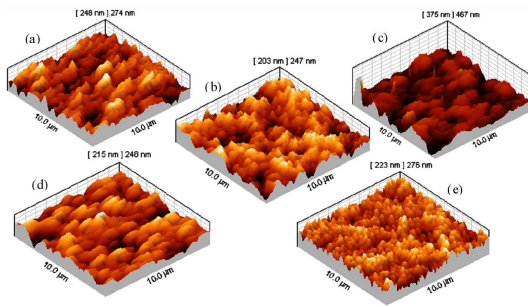


Fig. 4. AFM images of $Zn_xMn_{3-x}O_4$ ($x = 0.36$) films in (a) 300°C, (b) 400°C, (c) 500°C, (d) 600°C, (e) 800°C.

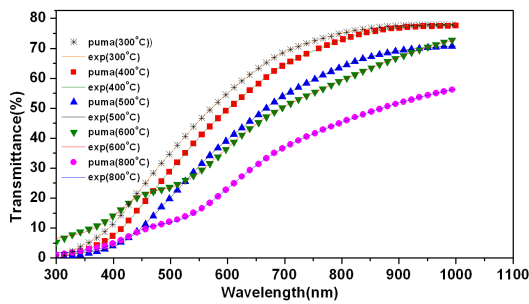


Fig. 5. Transmittance spectra of thin manganese oxide film by changes of annealing temperature.

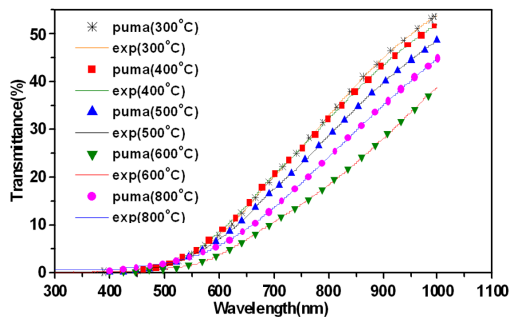


Fig. 6. Transmittance spectra of thin $Zn_xMn_{2-x}O_3$ ($x = 0.06$) film by changes of annealing temperature.

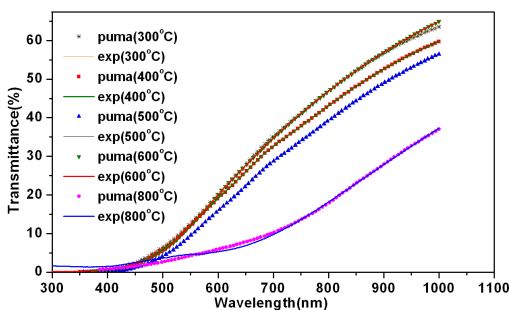


Fig. 7. Transmittance spectra of thin $Zn_xMn_{3-x}O_4$ ($x = 0.16$) film by changes of annealing temperature.

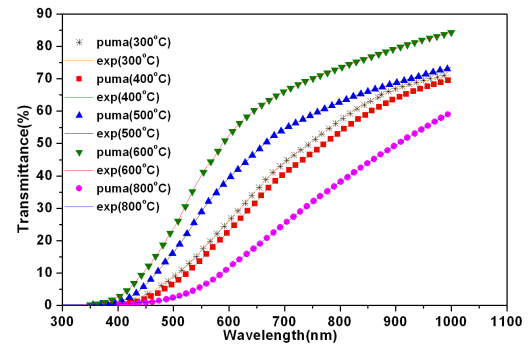


Fig. 8. Transmittance spectra of thin $Zn_xMn_{3-x}O_4$ ($x = 0.36$) film by changes of annealing temperature.

at different temperatures from 300°C to 800°C. The transmittance of the films was decreased when the annealing temperature increased from 300°C to 800°C. In Fig. 5 the transmittance for the films which were annealed at 300–500°C has significant differences compared to the others because of the MnO_2 phase transformation to Mn_2O_3 (from XRD can also be observed). When Zn was added in the precursor solution as $Zn_xMn_{2-x}O_3$ ($x = 0.06$) the transmittance of films exhibit complete Mn_2O_3 like phase at 600–800°C (from XRD) (Fig. 6). By increasing the Zn content as $Zn_xMn_{3-x}O_4$ the transmittance of films exhibit complete Mn_3O_4 like phase at 500–800°C (from XRD) (Figs. 7, 8). The transmittance of the manganese oxide thin films shows decreases in the visible region as a result of increasing annealing temperature. By increasing the Zn, the transmittance of films which were annealed at 500–800°C has considerable differences in comparison with the undoped films; because a structural transformation was observed from MnO_2 to Mn_2O_3 and Mn_3O_4 . Optical properties of manganese oxide thin films were determined by transmittance spectra and with optimization of data. When the annealed temperature increased from 300°C to 800°C, the thickness of manganese oxide thin films was decreased from 227 nm to 150 nm and it was also reduced from 207 to 154 nm in case of Zn doped sample ($x = 0.36$). The annealing temperature is found to have a significant influence on the optical properties of the films. The refractive index of a thin film is proportional to the density of the film.

The dispersion of refractive index of the films for different annealing temperature is represented in Figs. 9, 10. The high change of refractive index in the entire wavelength range is a potential in using of this material in reflective coating applications. The refractive index in all films increases when the annealing temperature increased from 300°C to 800°C. The refractive index for the films annealed at 600–800°C has significant differences compared to the others because of the MnO_2 phase transformation to Mn_2O_3 . By increasing the Zn, the refractive index for the films which were annealed at 500–800°C has remarkable differences compared to the undoped films; because a structural transformation was observed from MnO_2 and Mn_2O_3 to Mn_3O_4 .

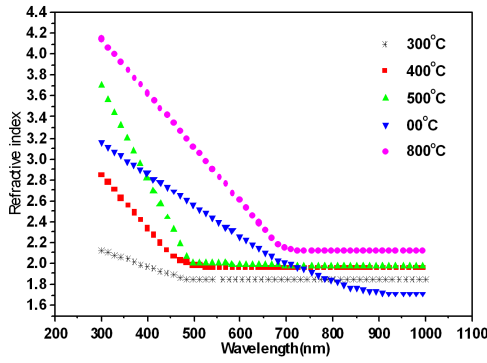


Fig. 9. Dispersion of refractive index of thin manganese oxide film by changes of annealing temperature.

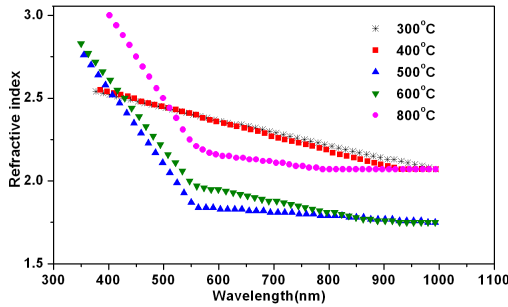


Fig. 10. Dispersion of refractive index of thin $Zn_xMn_{3-x}O_4$ ($x = 0.36$) film by changes of annealing temperature.

The spectral behaviour of extinction coefficient as a function of annealing temperature is shown in Figs. 11, 12. As shown in the figure, the extinction coefficient increases when the annealing temperature increases from 300 to 800 °C. The extinction coefficient for the films which were annealed at 600–800 °C is highly different from the other ones as a result of the MnO_2 phase transformation to Mn_2O_3 . By increasing the Zn, the refractive index of the films which were annealed at

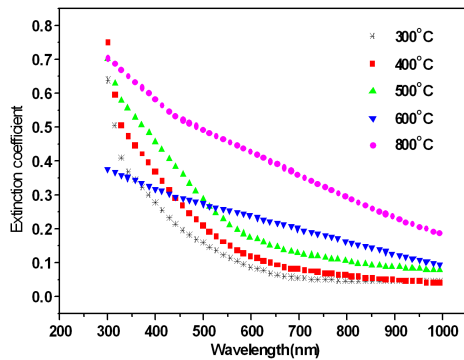


Fig. 11. Wavelength dependence of extinction coefficient for thin manganese oxide film by changes of annealing temperature.

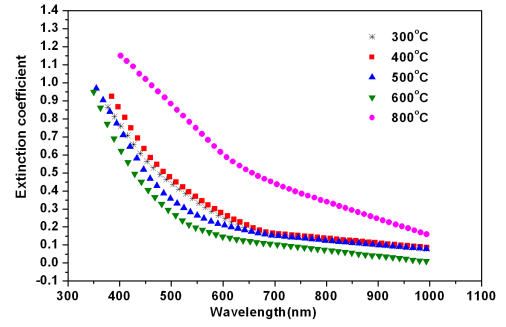


Fig. 12. Wavelength dependence of extinction coefficient for thin $Zn_xMn_{3-x}O_4$ ($x = 0.36$) film by changes of annealing temperature.

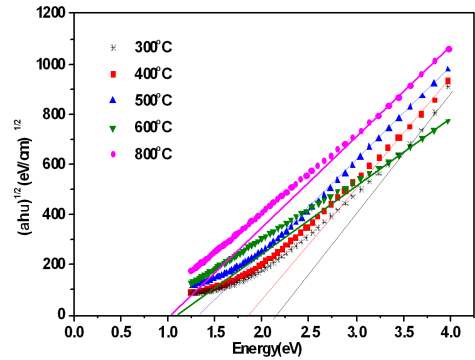


Fig. 13. Variation of $(\alpha h\nu)^{1/2}$ with photon energy for manganese oxide thin films with change of annealing temperature.

500–800 °C important differences are found compared to the undoped films; because a structural transformation was observed from MnO_2 and Mn_2O_3 to Mn_3O_4 . The absorption coefficient was calculated from the extinction coefficient

$$\alpha = \frac{4\pi k}{\lambda}. \tag{3}$$

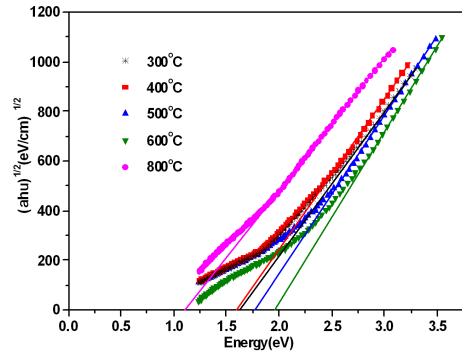


Fig. 14. Variation of $(\alpha h\nu)^{1/2}$ with photon energy for thin $Zn_xMn_{3-x}O_4$ ($x = 0.36$) film by changes of annealing temperature.

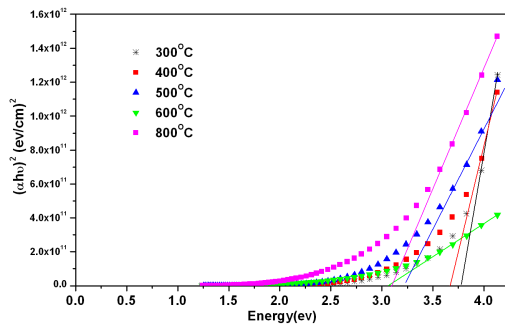


Fig. 15. Variation of $(\alpha h\nu)^2$ with photon energy for manganese oxide thin films with change of annealing temperature.

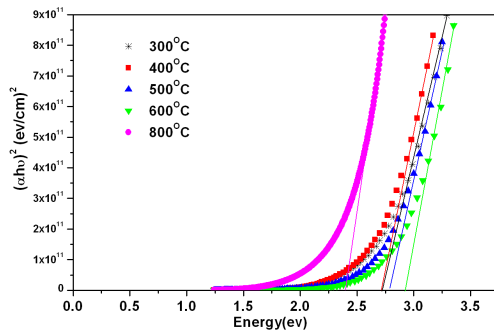


Fig. 16. Variation of $(\alpha h\nu)^2$ with photon energy for thin $Zn_xMn_{3-x}O_4$ ($x = 0.36$) film by changes of annealing temperature.

Then $(\alpha h\nu)^\eta$ was plotted as a function of $h\nu$, where $h\nu$ is the photon energy, and η is a constant that depends on the types of transitions. The values of 1/2 and 2 for η represent the indirect and direct transitions, respectively. No value for the direct energy gap of MnO_2 and indirect Mn_3O_4 have been reported. In this plot, the horizontal intercept represents the energy gap.

The plot of $(\alpha h\nu)^{1/2}$ and $(\alpha h\nu)^2$ with respect to $h\nu$ for indirect and direct optical transition of thin films is represented in Figs. 13–16. The direct and indirect band gaps of the films were decreased when the annealing temperature increased from 300 °C to 800 °C. The direct and indirect energy gaps for the films which were annealed at 600–800 °C show meaningful differences compared to the other due to the MnO_2 phase transformation to Mn_2O_3 . By increasing the Zn, the direct and indirect energy gaps of the films which were annealed at 500–800 °C present significant changes in comparison with the undoped films; a structural transformation which was observed from MnO_2 and Mn_2O_3 to Mn_3O_4 can be led to it.

4. Conclusions

In this work, thin films of MnO_2 , Mn_2O_3 and Mn_3O_4 were deposited by sol–gel using dip-coating technique and were annealed at 300 °C to 800 °C. We studied variations in the optical and structural properties of these thin films that resulted from changing the temperature of annealing. The annealing temperature expressively influences on optical and structural properties of the films. The optical band gap of the films decreases as a result of increasing the annealing temperature. Zn additive induces a structural transformation from Mn_2O_3 to Mn_3O_4 even under the same air-annealing condition. Optical properties of Mn_2O_3 , Mn_3O_4 , $Zn_xMn_{2-x}O_3$ ($x = 0.06$) and $Zn_xMn_{3-x}O_4$ ($x = 0.16$ – 0.36) were calculated by using the pointwise unconditioned minimization approach (PUMA) numerical approximation method from the experimental spectral transmittance. The calculated energy band gaps from optical data in this study are in good agreement with the value of other works [9, 16].

References

- [1] P. Fau, J.P. Bonino, A. Rousset, *Appl. Sci.* **78**, 203 (1994).
- [2] R.M. Vaalsetta, W.A. Pliskin, *J. Electrochem. Soc.* **114**, 944 (1967).
- [3] T. Seike, J. Nagai, *Sol. Energy Mater.* **22**, 107 (1991).
- [4] H. Yang, H. al-Britthen, A.R. Smith, J.A. Borchers, R.L. Cappelletti, M.D. Vaudin, *Appl. Phys. Lett.* **78**, 3860 (2001).
- [5] O. Nilsen, H. Fjellvåg, A. Kjekshus, *Thin Solid Films* **444**, 44 (2003).
- [6] S.A. Chambers, Y. Liang, *Surf. Sci.* **123**, 420 (1999).
- [7] L.W. Guo, H. Makino, H.J. Ko, Y.F. Chen, T. Hanada, D.L. Peng, K. Inaba, T. Yao, *J. Cryst. Growth* **955**, 227 (2001).
- [8] M. Chigane, M. Ishikawa, *J. Electrochem. Soc.* **148**, D96 (2001).
- [9] A.K.M. Farid Ul Islam, R. Islam, K.A. Khan, *Renew. En.* **30**, 2289 (2005).
- [10] R.M. Valletta, J. Makris, W.A. Pliskin, *Proc. Electron. Compon. Conf.* **16**, 31 (1966).
- [11] K. Wang Joo Kim, Young. Ran Park, *J. Crystal Growth* **270**, 162 (2004).
- [12] Y.J. Park, J.G. Kim, H.T. Chung, H.G. Kim, *Solid State Ionics* **130**, 203 (2000).
- [13] I. Chambouleyron, J.M. Martinez, A.C. Moretti, *Appl. Opt.* **36**, 1 (1997).
- [14] *JCPDS, International Centre for Diffraction Data* **41**, 1442 (1997).
- [15] C.O. Paiva-Santos, R.F.C. Marques, M. Jafelicci, L.C. Varandaa, *Powder Diffraction* **17**, 149 (2002).
- [16] M.F. Al-Kuhaili, *J. Vac. Sci. Technol.* **24**, 1746 (2006).